Synthesis and characterization of beta cyclodextrin nanosponges for N,N.diethyl-meta-toluamide complexation and theis application on polyester fabrics

DOI: https://doi.org/10.1016/j.reactfunctpolym.2017.08.008

Synthesis and characterization of β-cyclodextrin nanosponges for N,N-diethyl-meta-toluamide complexation and their application on polyester fabrics

Roberta Peila[a*], Pasquale Scordino[a], Dura Birhanu Shanko[a], Fabrizio Caldera[b], Francesco Trotta[b], Ada Ferri[a]

[a] Politecnico di Torino, Department of Applied Science and Technology, C.so Duca degli Abruzzi, 24, 10129 Torino, Italy

[b] Università di Torino, Department of Chemistry, Via Pietro Giuria, 7, 10125 Torino, Italy

*Corresponding author: roberta.peila@polito.it

Abstract

β-Cyclodextrin polymer, namely nanosponges (NSs), were synthesized using two cross-linkers: 1,1'-carbonyldiimidazole (CDI) and pyromellitic dianhydride (PMDA). The synthesized NSs were complexed with N,N-diethyl-meta-toluamide (DEET) and, after complex characterization, the NSs cross-linked with CDI were found more effective than those cross-linked with PMDA in terms of encapsulation efficiency and loading capacity. The CDI-NSs were dispersed in a polyacrylic resin, which was thermally polymerized on a polyester fabric surface. The fabric functionalization was evaluated through quantification of DEET extracted from the polyester fabrics, before and after three washing cycles. The results showed that encapsulation into NSs prolongs the persistence of DEET on polyester fabrics.

Keywords

β-cyclodextrin nanosponges; 1,1'-carbonyldiimidazole; Pyromellitic dianhydride; N,N-diethyl-meta-toluamide; Polyester fabrics

1. Introduction

Diseases transmitted by insects affect millions of people every year, most commonly in tropical and subtropical countries, where insects can be vehicle for many dangerous infections leading to death. Malaria is an example and mortality due to this infectious disease mainly occurs in infants and young children [1], [2]. Recently, Zika virus is alarming the international community because it has already spread to sixty-six countries and territories, and the World Health Organization has declared it a public health emergency of international concern, soliciting public health researchers to work on effective control strategies [3]. Zika is a mosquito-borne virus, and at present, no commercial vaccine is available; therefore, preventive measures should be taken to avoid the virus infection. The basic precautions are the same as those for any other mosquito-borne disease [4], among which use of insect repellents, such as N, N-diethyl-m-toluamide (DEET), is currently the most effective [5], [6], [7]. DEET shows repellence against mosquitoes, bugs and ticks. However, it cannot be effective for a long duration [8], [9]. Moreover, rubbing of garments, sweat, detergents, warm temperatures or high winds can considerably decrease the duration of effectiveness of repellent agents; therefore, it becomes necessary to reapply repellents frequently [10]. One way to overcome this problem is DEET encapsulation, which prolongs its persistence and, at the same time, results

in decreased absorption by skin, which is greatly appreciated because DEET may induce irritation when applied directly on skin [11], [12]. The use of novel polymer-based formulations represents a challenge that may guarantee effective protection against insect bites, long-lasting repellent action and minimal skin penetration [13]. In the case of insect protection, polymeric drug carriers are of great interest because they are considered a suitable strategy for time- and distribution-controlled drug delivery. The mechanism involved in controlled release requires polymers with a variety of physico-chemical properties. Thus, a wide range of polymers, including micro- and nanocapsules, have been used as potential carriers [14], [15]. Encapsulation allows maintaining the repellent effect for a longer period without exposing the individual to high dose of the product, which could lead to excessive dosage and adverse effects. The release of the encapsulated substance occurs by diffusion through the microstructure system or by its rupture [16], [17], [18].

Among many agents used for microencapsulation, cyclodextrins (CDs) have been the subject of numerous investigations. Because of their relatively hydrophobic cavity and hydrophilic outer shell, they can form host–guest complexes with suitable hydrophobic molecules. The formation of these complexes results in significant changes in the solubility and reactivity of the guest molecules, but without chemical modification. It is believed that hydrogen bonds and hydrophobic interactions are mainly responsible for drug encapsulation in the CD cavity. These compounds have been applied in many fields, e.g., food chemistry, cosmetics, textiles, organic coating, and pharmaceutical industries [19], [20], [21], [22]. By reacting CDs with suitable cross-linking agents, nanostructured hyper-crosslinked materials can be obtained [23], [24]. Nanosponges (NSs) are branched CD polymeric systems, which exhibit great potential in many different fields. Over the past decade, different varieties of NSs based on the type of CD and cross-linker have been tailored for specific applications. Romo et al. employed β-cyclodextrin polymers to extract phenols from aqueous solution [25]; Yinjuan et al. studied the release rate of model drug from β-CD incorporated hydrogel [26]. NS technology has been efficient in achieving solubilization, controlled release, permeability enhancement, improvement of bioavailability, etc. [27], [28], [29].

Microencapsulation technologies have been applied on textiles for insect protection. A number of studies have been reported on the efficacy of the insect repellent treatments of textiles. They have great potential for improving the longevity of highly volatile natural mosquito repellents and for developing highly efficient eco-friendly repellent textiles [30], [31], [32], [33]. When microencapsulation is used, suitable binders adhering to the fabrics and simultaneously supporting the mosquito repellent agents should be employed to fix the microcapsules on the fabric surface [34]. Specos et al. developed microcapsules containing citronella essential oil by complex coacervation and applied them to cotton fabrics to study the repellent efficacy of the materials. Textiles treated with microencapsulated citronella presented a higher and longer lasting protection than fabrics sprayed with an ethanol solution of free citronella oil [35].

Insect repellent textiles can also be produced by the incorporation of repellent agents inside the fiber or yarn before preparing the fabrics. In this case, the insect repellent agents are added during the spinning step of the fibers [36], and the process does not require any binder because the insect repellant is embedded in the fiber bulk rather than immobilized on the fiber surface.

In a study by İnceboz et al., the ability of β-CD cavity to form an inclusion complex with DEET molecule was demonstrated by DSC (Differential Scanning Calorimetry) analysis. The authors suggested a preferential 1:2 stoichiometry of the inclusion complex between β-CD and DEET [37]. Proniuk et al. described the inclusion complex formation between hydroxypropyl β-CD and DEET and found the association constant to be equal to 1286.5 M− 1 [38]. On the basis of these encouraging results, the present work aimed at creating a functionalized fabric incorporated with DEET-loaded NSs for protection against insect-borne diseases. N,N-diethyl-meta-toluamide (DEET) was complexed in β-CD-based NSs, dispersed in a polyacrylic resin for polyester fabric finishing to achieve insect repellence. The selected polyester fabric was intended for seat car covers as it has been reported that car cockpits, because of their carbon dioxide-enriched atmosphere,

attract mosquitoes [39]. Nevertheless, the process set up in the present work can be applied to different substrates as the polyacrylic resin used for binding the NSs on the fabric is of general textile use and not selective to polyester only.

Two synthesis routes have been followed by using two cross-linking agents: 1,1'-carbonyldiimidazole (CDI) and pyromellitic dianhydride (PMDA). Moreover, DEET complexation was carried out according to two different methods: DEET was complexed with the β-CD cavities before cross-linking (pre-loaded NSs) or DEET was complexed with the NSs after cross-linking (post-loaded NSs). A specific aim of the work was to assess which complexation method was more effective in terms of DEET encapsulation efficiency, loading capacity, and washing durability.

2. Experimental

2.1. Materials

β-CD was a gift of Roquette Italia (Italy). CDI, triethylamine (Et3N), N,N-dimethylformamide (DMF), PMDA, dimethylsulfoxide (DMSO) and DEET were supplied by Sigma-Aldrich (Italy) and used as received. Fig. 1 shows the molecular structure of DEET.

Knitted 100% PET, polyester fabrics (240 g/m2), were kindly supplied by Sinterama s.p.a. (Italy). The polyacrylic resin Dicrylan AC01 was kindly supplied by Huntsman International.

2.2. Synthesis of NSs

Different types of NSs were synthetized, under different process conditions in terms of temperature, type and concentration of cross-linker and DEET complexation method.

2.2.1. Synthesis of preloaded DEET-CDI-NSs

A known amount of β-CD (Table 1) was dissolved in a proper volume of DMF (50 mL) at room temperature in a round bottom flask, under magnetic stirring, until a clear solution was observed. Subsequently, the selected amount of DEET corresponding to 1:10, 1:1, 5:1, and 10:1 β-CD:DEET molar ratio was added and the solution was kept under stirring for 1 h to allow DEET complexation. After adding the amount of CDI corresponding to 1:4 or 1:8 β-CD:CDI molar ratio, the suspension was heated to 40 °C or 70 °C, so that the cross-linking reaction between CDI and β-CD occurred. The product of the synthesis was an organogel. The specific synthesis conditions for each batch are summarized in Table 1, and the reaction scheme is shown in Fig. 2 – Scheme 1. The reacted mixture was then cooled to room temperature and rinsed with deionized water, thus obtaining a solid product recovered by filtration under vacuum. Finally, the NSs were dried, ground manually, and sieved through a 70-μm mesh to obtain a homogeneous powder.

2.2.2. Synthesis of preloaded DEET-PMDA-NSs

PMDA-NS synthesis was similar to that of CDI-NSs, except for presence the catalyst (tryethylamine) used to accelerate the cross-linking reaction in PMDA-NS synthesis. The PMDA-NS synthesis conditions are shown in Table 1. A known amount of β-CD was dissolved in 50 mL DMSO at room temperature in a round bottom flask. The amount of DEET corresponding to 1:1, 5:1, or 10:1 β-CD:DEET molar ratio was then added and the solution was kept under stirring for 1 h to allow DEET complexation into β-CD cavities. Subsequently, the

required amount of PMDA was added to the mixture. Tryethylamine in molar ratio 1:1 with PMDA was added as catalyst. After the organogel was formed, the mixture rinsed with deionized water under vacuum filtration. The solid product was then dried, ground manually, and sieved through a 70-µm mesh to obtain a homogeneous powder. The reaction scheme is presented in Fig. 2 – Scheme 2.

2.2.3. Synthesis of postloaded CDI- and PMDA-NSs

For comparison purposes, plain CDI-NSs and PMDA-NSs were prepared according to the same procedures described in the above two paragraphs, but without the addition of DEET. The synthesis details for each batch are given in Table 1.

For DEET complexation, the plain NSs and DEET were suspended in acetone with an excess of DEET. The mixture was kept under magnetic stirring for 24 h. Acetone was then removed by vacuum filtration, and the powder obtained was dried, ground manually, and sieved through a 70-µm mesh to obtain homogenous NS powder.

2.3. Functionalization of polyester fabrics with the synthesized CDI-NSs

The polyester fabrics were scoured in 5 g/L standard detergent ECE solution at 95 °C for 35 min. Subsequently, the finishing bath was prepared by dosing 30 g/L polyacrylic resin (Dicrylan AC01) and 10% owf (on weight of fibers) of synthesized DEET-loaded CDI-NSs in an aqueous bath at 30 °C. As discussed in the results section, PDMA-NSs were far less capable of entrapping DEET and were excluded from fabric functionalization. The fabric was dipped in the finishing bath for 30 min under stirring. Afterwards, two different procedures were followed for fabric impregnation. The first one was a conventional pad-dry-cure process, with fabric squeezing through rollers at a pressure of 1 bar, drying in an oven at 60 °C until constant weight, and subsequently heating at 125 °C for 7 min for resin curing.

In the second procedure, after impregnation into the DEET-CDI-NSs/acrylic resin suspension, the fabric was directly placed in the oven at 60 °C without squeezing until constant weight and then heated at 125 °C for 7 min for resin curing.

For comparison purpose, a finishing bath with 30 g/L polyacrylic resin and 0.3 g/L free DEET was prepared and a fabric sample was treated with resin plus DEET, without CDI-NSs, under the same process conditions. Free DEET concentration was selected to have the same DEET quantity as that encapsulated in the CDI-NSs during the synthesis with β-CD/DEET molar ratio 5:1.

2.4. Washing tests

After functionalization, the PET fabrics were washed at 40 °C for 40 min in a 2-g/L ECE standard detergent solution. The washings were performed in the Beaker dyeing Labomat equipment (Mathis, Switzerland) with a fabric-to-bath ratio 1:40, at a revolving speed of 55 rpm with alternating clockwise and anticlockwise rotations.

2.5. Characterization techniques

2.5.1. Soxhlet extractions

DEET-loaded NSs and the treated PES fabrics were subjected to Soxhlet extraction for quantification purposes for 3 h in ethanol. The treated fabrics were Soxhlet extracted before and after the washing tests.

2.5.2. HPLC analysis

HPLC analysis of the extracts was performed using a Waters separation module 2695,2998 Photodiode Array Detector and C18 column. The mobile phase was composed of 43% water and 57% methanol. A flow rate of 1 mL/min, column temperature of 25 °C, injection volume of 20 µL, and retention time of 15 min were set. Before the analysis, the solutions were filtered through a 0.22-µm filter. Calculations were made according to the following calibration line (Eq. (1)):

$$A = 49000 * C + 20252 \qquad (1)$$

where A is the peak area as given by the instrument and C is the corresponding solution concentration.

2.5.3. Thermogravimetric analysis

Thermogravimetric analysis was performed using TA Instrument TGA2050. 10 mg samples were used for the analysis. The furnace was heated from 40 °C to 700 °C at a heating rate of 10 °C/min. The analysis was performed in inert atmosphere under a 100 mL/min nitrogen flow rate.

2.5.4. SEM analysis

SEM images were obtained using a Leica Electron Optics 435 VP instrument (UK) with an acceleration voltage of 10 kV.

2.5.5. BET analysis

BET analysis was performed using a Micrometrics ASAP 2020 N2 physi-sorption machine. Before the analysis, the samples were heated at 120 °C for 2 h to eliminate the potentially physically adsorbed molecules. Nitrogen adsorption–desorption isotherm was measured at 77 K.

2.5.6. NMR analysis

Solid-state NMR spectra were acquired using a Jeol ECZR 600 instrument, operating at 600.17 and 150.91 MHz for ^{1}H and ^{13}C nuclei, respectively. Powder samples were packed into cylindrical zirconia rotors with an OD of 3.2 mm and volume of 60 µL. A certain amount of the samples was collected from each batch and used without further preparations to fill the rotor. ^{13}C CPMAS spectra were acquired at a spinning rate of 20

kHz using a ramp cross-polarization pulse sequence with a contact time of 3.5 ms, a 90° ^{1}H pulse of 2.189 µs, (optimized) recycle delays between 1 and 2 s, and the number of scans between 1000 and 20,000, depending on the sample. For every spectrum, a two-pulse phase modulation decoupling scheme with a radiofrequency of 108.5 kHz was used. The chemical shift scale was calibrated through the methylenic signal of external standard glycine (at 43.7 ppm).

2.5.7. FTIR analysis

Perkin Elmer Spectrum 100 was used in attenuated total reflectance (ATR) mode with a diamond crystal in the region from 4000 to 650 cm^{-1}. ATR-FTIR spectra of plain NSs, pure DEET, and DEET-loaded NSs were collected. Each spectrum was scanned 8 times with a resolution of 4 cm^{-1}.

3. Results and discussions

3.1. DEET encapsulation efficiency and loading capacity of synthesized NSs

Encapsulation efficiency (EE) and loading capacity (LC) are expressed by Eqs. (2), (3), respectively.

$$EE\% = \frac{M_{encaps\_DEET}}{M_{used\_DEET}} * 100 \qquad (2)$$

$$LC = \frac{M_{encaps\_DEET}}{M_{NS}} \qquad (3)$$

where Mencaps_DEET is the amount of DEET in the NSs (estimated by HPLC analysis), M_{used_DEET} is the initial amount of DEET added in the process (estimated gravimetrically), and M_{NS} is the amount of NSs from which DEET was extracted (estimated gravimetrically).

The results are shown in Table 2.

From the comparison between the EE of CDI- and PMDA-NSs, it can be concluded that CDI-NSs have a much higher EE. This result may be ascribed to PMDA chemical structure, which gave the NSs a more polar character than CDI. The polarity of PMDA-NSs brings a partially negative charge on the surface, which prevents the interaction with the functional groups of DEET molecule. Moreover, it causes a pronounced swelling of the NSs when in contact with water. The swelling facilitates DEET loss during the rinsing step. Finally, the more rigid and compact structure of CDI-NSs than that of PMDA-NSs, deriving from low molecular weight of the cross-linking bridges, helps to limit the diffusion and loss of entrapped DEET molecules.

With regard to CDI-NSs, the maximum EE and LC were found in the case of CDI-NSs synthesized with large excess of DEET with respect to β-CD (10:1). However, it is worth observing that EE was small if compared with the excess of DEET used in the process: in fact, with 50 times more DEET (β-CD:DEET 1:10 vs. 5:1), EE slightly increased from 42.3% to 49.3%. This implies that in the case of large excess of DEET, the encapsulation was largely inefficient and great amounts of DEET were depleted during the process. As an overall consideration, 5:1 can be considered as the optimal β-CD:DEET molar ratio because the EE seemed to reach a maximum regardless of the other operative parameters.

The effect of β-CD:CDI molar ratio is controversial: with the increase in β-CD:CDI molar ratio from 1:4 to 1:8, EE improved when β-CD was in excess with respect to the amount of DEET (from 33.0% to 42.3% in the

case of 5:1 β-CD:DEET and from 26.9% to 35.5% in the case of 10:1 β-CD:DEET); however, it decreased in the case of 1:1 β-CD:DEET molar ratio (from 23.8% to 16.2%). It can be supposed that CDI favored the formation of a nanoporous, three-dimensional structure with more cavities that can host large amounts of DEET; however, this effect was hindered by DEET because it interfered with the cross-linking reaction. Therefore, when β-CD:DEET was 1:1, the degree of cross-linking was lower than in the cases of 5:1 or 10:1 β-CD:DEET. As shown later, the disturbance of DEET in the cross-linking reaction was confirmed by FTIR analysis where the CO signal of the cross-linking bridge was attenuated in DEET-loaded CDI-NSs with respect to plain CDI-NSs, and this was probably the symptom of a lower degree of cross-linking of loaded NSs with respect to plain ones.

When DEET was post-loaded after synthesis, EE was much lower than in the case of DEET- preloaded NSs synthesized under the same conditions (20.9% vs. 42.3%, respectively). In the case of preloaded NSs, DEET was entrapped in the organogel during its formation, whereas in the case of post-loaded NSs, DEET must diffuse into the surface and inside the porous NS structure before complexation into the NSs. Diffusion in porous media is notoriously a slow process; therefore, more free DEET, which can be easily removed by rinsing, was likely present in post-loaded NSs than in preloaded ones. A more intimate contact between DEET and NSs could result also in a stronger and more durable complex in the case of preloaded than postloaded NSs, and this hypothesis was confirmed by the washing test results, which are presented in Section 3.6.

Finally, it can be observed that temperature did not substantially affect EE. PMDA-NSs were excluded from further investigation because they exhibited too low EE.

3.2. Morphological and thermal characterization of DEET-loaded CDI-NSs

As shown in Fig. 3, CDI-NSs have irregular microporous structures with a rough surface.
Table 3 reports the BET analysis performed on CDI-NSs. The specific surface area Sbet, the specific porous volume Vp, and the mean pore diameter Dp are reported. BET analysis evidenced that CDI-NSs have a small specific surface area. This result is in accordance with the literature, which reports that CD polymers cross-linked with small linkers have little framework porosity, except the inherent cavities of CD, thereby leading to a small specific surface area [40], [41]. This result suggests that DEET adsorption on the CDI-NS surface is negligible, and complexation in the CD inner cavities is the main route for DEET incorporation.

Fig. 4 shows the TGA thermograms of DEET, plain CDI-NSs, and DEET-loaded CDI-NSs with 1:10 and 5:1 β-CD:DEET ratios. A 3–5% weight loss between 30 °C and 110 °C occurred for the NSs, both for the loaded and plain ones, due to the evaporation of water molecules from the nanoporous structure. Furthermore, plain and DEET-loaded NSs started to degrade at about 150 °C following two degradation steps, with a main weight loss starting at 300 °C. The thermograms of DEET-loaded CDI-NSs, in particular, the curve of CDI-NSs loaded with an excess of DEET, did not show any weight loss corresponding to DEET evaporation/decomposition temperature. This observation indicated that the formation of DEET/CDI-NSs complexes thermally protected the active principle. These findings are in agreement with the literature, which reports that encapsulation in CD improves the thermal stability of the guest molecules [42], [43]. At 700 °C, 8% of CDI-NSs char remained visible, thus indicating the formation of amorphous carbon residue.

3.3. FTIR analysis

The FTIR spectra of DEET, plain CDI-NSs, and DEET-loaded CDI-NSs, are shown in Fig. 5. The FTIR spectrum of DEET showed the characteristic absorption bands of the main DEET functional groups: the CH stretching vibrations were visible at 2971–2933 cm^{-1} and the CO stretching at 1626–1584 cm^{-1}. The spectrum of plain

NSs showed intense vibration bands in the region 3000–3500 cm^{-1} due to OH stretching, at 2850–3000 cm^{-1} due to CH stretching, at 1700 cm^{-1} due to CO stretching, and at 1150 and 1082 cm^{-1} due to the C-O-C absorption bands typical of polysaccharides. The FTIR spectrum of DEET-loaded CDI-NSs did not show a direct evidence of DEET absorption peaks, whose bands were almost completely unnoticed because of the very intense and broad CDI-NS bands, which were greatly affected by molecular complex formation. This observation indicates that DEET main bands were weakened when they interacted with the CDI-NS structure and that DEET molecules were located inside the CDI-NSs; hence, their IR signals were hidden. This is in agreement with the results of Yaser et al., who encapsulated curcumin in Chlorella [44]. They noticed that curcumina typical signals were hidden in the FTIR spectrum of curcumina/chlorella complex. Only at 2981 cm^{-1}, the peak in the loaded CDI-NSs evidenced a sharper profile than plain NSs, and this may be considered a direct evidence of DEET presence, due to CH stretching. Moreover, the strong signal at 1700 cm^{-1}, due to CO stretching of the cross-linking bridge, was weaker in loaded CDI-NSs than in plain ones. This might be due to the presence of DEET, which decreased the degree of cross-linking in the DEET-loaded CDI-NSs compared with that in the plain ones.

3.4. NMR analysis of DEET-loaded CDI-NSs

Fig. 6 shows the ^{13}C CPMAS SSNMR spectra of plain CDI-NSs (1:8) and DEET-loaded CDI-NSs (1:8). In the spectrum of the loaded sample, several signals, different from the characteristic peaks of NSs, were observed, in agreement with the typical chemical shifts of the ^{13}C atoms of DEET. The proposed assignments of ^{13}C CPMAS SSNMR signals are reported in the table below the spectrum. The signals ascribed to DEET carbons are a direct evidence of DEET presence entrapped in the NS structure. Moreover, a low signal at 31.1 ppm was seen; this is likely due to the presence of an impurity in the sample.

3.5. DEET quantification of loaded NS fabrics

CDI-NSs with 1:8 β-CD:CDI molar ratio and 5:1 or 1:10 β-CD:DEET molar ratio were selected for fabric functionalization. Moreover, plain CDI-NSs loaded with DEET after the synthesis (post-loaded CDI-NSs) were used. Finally, a fabric sample was treated with free DEET and polyacrylic resin to evaluate the effect of complexation on the treatment duration.

The results are displayed in Fig. 7 - A, where the percentage of DEET retained on the fabric refers to the amount of DEET found on the fabric with respect to the amount of DEET added in the finishing bath. Two mechanisms for DEET loss were identified in the entire process: (1) DEET was lost in the NS synthesis, as demonstrated by the EE hardly exceeding 40% and (2) DEET was lost in the fabric treatment, partly lost in the finishing bath and partly released during curing at high temperature. Fig. 7 – A shows that the amount of DEET lost in step (2) is higher than that lost in step (1). However, large differences in the amount of DEET retained in the treated fabric were found in the case of padding-with-squeezing. A maximum 10% of DEET initially loaded in the CDI-NSs was found on the fabric, while the percentage increased up to 60% without squeezing: with the increase in the amount of resin added, more DEET was deposited on the fabric surface during padding-without-squeezing. However, fabric flexibility and touch was acceptable, despite the greater amount of polymerized resin on top of the fabric surface. It is worth mentioning that PET fabric was quite heavy (240 $g \cdot m^{-2}$) and not very pliable as it was intended for automotive applications. In this case, stiffening caused by the resin was a minor concern.

No substantial difference (in terms of DEET retained on the fabrics) between pre- or post-loaded NSs in the padding-with-squeezing method was observed, while a large difference was observed in padding-without-squeezing. As mentioned before, the extent of DEET complexation into the NSs was approximately double

in the case of preloaded than that in post-loaded NSs. After fabric functionalization, this proportion was not conserved: in padding-with-squeezing, DEET retained on the fabric was approximately the same in the case of preloaded and post-loaded NSs, whereas in padding-without-squeezing, the amount of DEET in preloaded NSs was about triple than that in post-loaded NSs. A possible explanation lies in the release of encapsulated DEET from the NSs in the finishing bath, which could be more consistent in the case of post-loaded NSs than in preloaded NSs. In other words, when DEET-loaded NSs were dispersed in the resin bath, some DEET was released, and the extent of DEET release could be reasonably greater in the case of post-loaded NSs than that in the preloaded NSs because the DEET–NSs interactions are weaker on average in post-loaded NSs than in preloaded NSs.

In padding-with-squeezing, DEET released from the NSs in the finishing bath was mostly squeezed out from the fabric. On the contrary, in the case of padding-without-squeezing, the DEET released from the NSs was left on the fabric and partly depleted during curing. In padding-without-squeezing, preloaded NSs resulted in greater DEET retention on the fabric than post-loaded NSs because of stronger DEET–NSs complex interactions. This hypothesis was supported by the observation that fabrics treated with post-loaded NSs or free DEET retained approximately the same amount of DEET at the end of the functionalization process, while fabrics treated with preloaded NSs retained triple the amount.

The amount of DEET found on the fabric was maximum 60% of that encapsulated in CDI-NSs. This confirms that the functionalization removes a considerable fraction of DEET. The amount retained on the fabric treated with post-loaded NSs was 20%, and with free DEET was 15%. These results show that CD complexation during the synthesis process produces NSs, where DEET inclusion results in stronger interactions with the NS structure. The CDI-NSs loaded with a large excess of DEET during the synthesis evidenced a greater amount of DEET loss. The large excess of DEET may have formed large DEET agglomerates in the three-dimensional NS structure; therefore, weaker interactions may have been formed between DEET and NSs. The data obtained indicate a DEET concentration of 0.7 mg/g in the case of preloaded CDI-NSs (β-CD:DEET 5:1) and 0.2 mg/g in the case of post-loaded CDI-NSs on polyester fabric.

3.6. Washing durability

The functionalized fabrics were subsequently washed to test the durability of the functionalization. Fig. 7 - B reports the amount of DEET extracted from each fabric.

The results confirm that polyester fabrics treated with loaded CDI-NSs during the synthesis and with a β-CD:DEET molar ratio 5:1 confer a stronger interaction between the NSs and DEET. As a consequence, the fabrics functionalized with this type of NSs maintain a higher percentage of residual DEET after washing.

4. Conclusions

β-CD-based insect repellent NSs were synthesized from the reaction between β-CD and two cross-linking agents: CDI and PMDA. The NSs were complexed with DEET insect repellent during or after the synthesis. Among the synthesized NSs, CDI-NSs preloaded with 5:1 M ratio of β-CD:DEET showed the best performance in terms of EE and were selected for polyester fabric functionalization. A thermocurable polyacrylic resin was used to promote adhesion of the NSs on the polyester fabric. Even though the fabric finishing proved to be a source of DEET loss, an acceptable percentage of DEET retained on the fabric was observed in the case of CDI-NSs preloaded with 5:1 M ratio of β-CD:DEET, which showed stronger interactions between DEET and NSs. This result was confirmed by the washing test, after which DEET-preloaded CDI-NSs still retained about 20% of DEET initially added during fabric functionalization. The work

has shown the possibility to prepare insect repellent polyester fabrics that might have the potential of improving the lifetime effectiveness of insect repellents.

Acknowledgments

The authors wish to thank Roquette Italia s.p.a. (Cassano Spinola, Italy) for kindly providing β-CD that was used in this study. The authors would like to thank Prof. Roberto Gobetto (Department of Chemistry, University of Torino) and his research team for the NMR analysis, Prof. Nunzio Russo and Marco Piumetti of Politecnico di Torino for BET analysis.

References

[1] B. Solomon, F. Sahle, T. Gebre-Mariam, K. Asres, R.H.H. Neubert Microencapsulation of citronella oil for mosquito-repellent application: formulation and in vitro permeation studies Eur. J. Phar. Biopharm., 80 (2012), pp. 61-66, 10.1016/j.ejpb.2011.08.003

[2] M.A. Tolle Mosquito-Borne Diseases Curr Problems Pediatric Adolescent Health Care 39 (2009), pp. 97-140 http://dx.doi.org/10.1016/j.cppeds.2009.01.001

[3] http://www.cdc.gov/media/releases/2016/s0208-zika-eoca-activation.html

[4] N. Arora, A.K. Banerjee, L.M. Narasu Zika virus: an emerging arboviral disease Fut Vir, 11 (6) (2016), pp. 395-399

[5] E. Lupi, C. Hatz, P. Schlagenhauf The efficacy of repellents against Aedes, Anopheles, Culex and Ixodes spp. - a literature review Doc. Travel Med. Inf. Dis., 3 (6) (2013), pp. 374-411, 10.1016/j.tmaid.2013.10.005

[6] C. Peterson, J. Coats Insect repellents –past, present and future Pestic. Outlook, 12 (4) (2001), pp. 154-158, 10.1039/B106296B

[7] A. Abd-Ella, M. Stankiewicz, K. Mikulska, ..., D. Servent, B. Lapied The repellent DEET potentiates carbamate effects via insect muscarinic receptor interactions: an alternative strategy to control insect vector-borne diseases PLoS ONE, 10 (5) (2015), 10.1371/journal.pone.0126406

[8] J.H. Diaz Chemical and plant-based insect repellents: efficacy, safety, and toxicity wilderness Environ. Med., 27 (1) (2016), pp. 153-163, 10.1016/j.wem.2015.11.007

[9] T.M. Katz, J.H. Miller, A.A. Hebert Insect repellents: historical perspectives and new developments J. Am. Acad. Dermatol., 58 (5) (2008), pp. 865-871, 10.1016/j.jaad.2007.10.005

[10] M. Brown, A.A. Hebert Insect repellents: an overview J. Am. Acad. Dermatol., 36 (2) (1997), pp. 243-249, 10.1016/S0190-9622(97)70289-5

[11] P.J. Robbins, M.G. Cherniack Review of the biodistribution and toxicity of the insect repellent n, n-diethyl-m-toluamide (Deet) J. Toxicol. Environ. Health, 18 (4) (1986), pp. 503-525, 10.1080/15287398609530891

[12] D.L. Sudakin, T. Osimitz DEET Hayes' Handbook of Pesticide Toxicology (2010), pp. 2111-2125, 10.1016/B978-0-12-374367-1.00098-7

[13] H. Qiu, J.W. McCall, H. Won Jun Formulation of topical insect repellent N,N-diethyl-m-toluamide (DEET): vehicle effects on DEET in vitro skin permeation Int. J. Pharm., 163 (1–2) (1998), pp. 167-176, 10.1016/S0378-5173(97)00379-7

[14] T.N. Barradas, J.P. Senna, E.R. Júnior, C.R.E. Mansur Polymer-based drug delivery systems applied to insects repellents devices: a review Curr. Drug Deliv., 13 (2) (2016), pp. 221-235, 10.2174/1567201813666151207110515

[15] G. Vilar, J. Tulla-Puche, F. Albericio Polymers and drug delivery systems Curr. Drug Deliv., 9 (4) (2012), pp. 367-394, 10.2174/156720112801323053

[16] R. N'Guessan, B.G.J. Knols, C. Pennetier, M. Rowland DEET microencapsulation: a slow-release formulation enhancing the residual efficacy of bed nets against malaria vectors Trans. R. Soc. Tropic. Med. Hyg., 102 (3) (2008), pp. 259-262, 10.1016/j.trstmh.2007.10.012

[17] Kumar B. Pavan, Chandiran I. Sarath, B. Bhavya, M. Sindhuri Microparticulate grug delivery system: a review Indian J. Pharm. Sci. Res., 1 (1) (2011), pp. 19-37

[18] H. Ichiura, K.-I. Yamamoto, Y. Ohtani Low temperature-dependence of N,N-dimethyl-3-methylbenzamide (DEET) release from a functional paper containing paraffin-DEET composites prepared using interfacial polymerization Chem. Eng. J., 245 (2014), pp. 17-23, 10.1016/j.cej.2014.02.019

[19] N. Kistamah, C.M. Carr, S. Rosunee Surface chemical analysis of tencel and cotton treated with a monochlorotriazinyl (MCT) β-cyclodextrin derivative J. Mater. Sci. (2006), pp. 2195-2200, 10.1007/s10853-006-7183-6

[20] R. Holm, N.E. Olesen, S.D. Alexandersen, B.N. Dahlgaard, P. Westh, H. Mu Thermodynamic investigation of the interaction between cyclodextrins and preservatives - application and verification in a mathematical model to determine the needed preservative surplus in aqueous cyclodextrin formulations Eur. J. Pharm. Sci., 87 (2016), pp. 22-29, 10.1016/j.ejps.2015.09.011

[21] N. De Lima Petito, D. Da Silva Dias, V.G. Costa, D.Q. Falcão, K.G. De Lima Araujo Increasing solubility of red bell pepper carotenoids by complexation with 2-hydroxypropyl-β-cyclodextrin Food Chem., 208 (2016), pp. 124-131, 10.1016/j.foodchem.2016.03.122

[22] L. Leclercq Smart medical textiles based on cyclodextrins for curative or preventive patient care Act. Coat. Smart Text. (2016), pp. 391-427, 10.1016/B978-0-08-100263-6.00017-4

[23] K. Hiroyuki, N. Taichi Polymerization of β-cyclodextrin with 1,2,3,4-butanetetracarboxylic dianhydride: synthesis, structural characterization, and bisphenol A adsorption capacity React. Funct. Polym., 73 (6) (2013), pp. 1096-1102

[24] Z. Jun, L. Tian-Tian, C. Guo An effective β-cyclodextrin polyurethane spherical adsorbent for the chromatographic enrichment of corilagin from Phyllanthus niruri L. extract React. Funct. Polym., 102 (2016), pp. 119-129

[25] A. Romo, F.J. Penas, J.R. Isasi, I.X. Garcia-Zubiri, G. Gonzales-Gaitano Extraction of phenols from aqueous solutions by β-cyclodextrin polymers. Comparison of sorptive capacities with other sorbents React. Funct. Polym., 68 (1) (2008), pp. 406-413

[26] H. Yinjuan, L. Mingzhu, W. Lu, G. Chunmei, X. Shanshan A novel triple-responsive poly(3-acrylamidephenylboronic acid-co-2-(dimethylamino) ethyl methacrylate)/(β-cyclodextrin-epichlorohydrin)hydrogels: synthesis and controlled drug delivery React. Funct. Polym., 71 (6) (2011), pp. 666-673

[27] S. Swaminathan, R. Cavalli, F. Trotta Cyclodextrin-based nanosponges: a versatile platform for cancer nanotherapeutics development Wiley Interdiscip. Rev. Nanomed. Nanobiotechnol., 8 (4) (2016), pp. 579-601, 10.1002/wnan.1384

[28] F. Trotta, F. Caldera, R. Cavalli, A. Mele, C. Punta, L. Melone, F. Castiglione, B. Rossi, M. Ferro, V. Crupi, D. Majolino, V. Venuti, D. Scalarone Synthesis and characterization of a hyper-branched water-soluble β-cyclodextrin polymer Beilstein J. Org. Chem., 10 (2014), pp. 2586-2593, 10.3762/bjoc.10.271

[29] M. Irfan, M. Seiler Encapsulation using hyperbranched polymers: from research and technologies to emerging applications Ind. Eng. Chem. Res., 49 (3) (2010), pp. 1169-1196, 10.1021/ie900216r

[30] S.D. Banks, N. Murray, A. Wilder-Smith, J.G. Logan Insecticide-treated clothes for the control of vector-borne diseases: a review on effectiveness and safety Med. Vet. Entomol., 28 (1) (2014), pp. 14-20

[31] J.C. Forgearini, C.B. Michalowski, E. Assumpcao, A.R. Pohlmann, S.S. Guterres Development of an insect repellent spray for textiles based on permethrin-loaded lipid-core nanocapsules J. Nanosci. Nanotechnol., 16 (2) (2016), pp. 1301-1309

[32] J.M. Souza, A.L. Caldas, S.D. Tohidi, R. Fangueiro, A. Zille Properties and controlled release of chitosan microencapsulated limonene oil Braz. J. Pharm., 24 (6) (2014), pp. 691-698

[33] A. Hebeish, S.M. El-Sawy, M. Ragaei, M.K. El-Bisi, F.A. Abdel-Mohdy New textiles of biocidal activity by introduce insecticide in cotton-poly (GMA) copolymer containing β-CD Carbohydr. Polym., 99 (2014), pp. 208-217

[34] S. Marinkovic, D. Bezbradica, P. Skundric Microencapsulation in the textile industry Chem. Ind. Chem. Eng. Q., 12 (2006), pp. 58-62

[35] M.M. Specos, J.J. García, J. Tornesello, P. Marino, M.D. Vecchia, M.V. Tesoriero, L.G. Hermida Microencapsulated citronella oil for mosquito repellent finishing of cotton textiles Trans. R. Soc. Trop. Med. Hyg. (2010), 10.1016/j.trstmh.2010.06.004

[36] L. Van Langenhove, R. Paul Insect Repellent Finishes for Textiles, Functional Finishes Tex: Improving Comfort, Performance and Protection Elsevier Inc. (2014), pp. 333-360

[37] T. İnceboz, G. Erkan, G.C. Türkoğlu, A.M. Sarıışık, S. Bakırcı, S. Üner, A. Üner In-vivo and in-vitro tick repellent properties of cotton fabric Text. Res. J., 85 (2015), pp. 2071-2082, 10.1177/0040517515578326

[38] S. Proniuk, B.M. Liederer, S.E. Dixon, J.A. Rein, M.A. Kallen, J. Blanchard Topical formulation studies with DEET (N,N-diethyl-3-methylbenzamide) and cyclodextrins J. Pharm. Sci., 91 (2002), pp. 101-110, 10.1002/jps.10009

[39] J. Walton Olfactory carbon dioxide detection by insects and other animals Mol. Cell, 35 (2) (2013), pp. 87-92, 10.1007/s10059-013-0035-8

[40] H. Li, B. Meng, S.-H. Chai, H. Liu, S. Dai Hyper-crosslinked β-cyclodextrin porous polymer: an adsorption-facilitated molecular catalyst support for transformation of water-soluble aromatic molecules Chem. Sci., 7 (2) (2016), pp. 905-909

[41] F. Trotta, F. Caldera, R. Cavalli, M. Soster, C. Riedo, M. Biasizzo, Barretta G. Uccello, F. Balzano, V. Brunella Molecularly imprinted cyclodextrin nanosponges for the controlled delivery of L-DOPA: perspectives for the treatment of Parkinson's disease Exp. Opin. Drug Deliv., 13 (2016), pp. 1671-1680, 10.1080/17425247.2017.124839

[42] A. Calderini, F.B.T. Pessine Synthesis and characterization of inclusion complex of the vasodilator drug minoxidil with β-cyclodextrin J. Incl. Phenom. Macrocycl. Chem., 60 (2008), pp. 369-377, 10.1007/s10847-007-9387-z

[43] J.Y. Tsao, C.P. Wu, H.H. Tsai, K.C. Peng, P.Y. Lin, S.Y. Su, L.D. Chen, F.J. Tsai, Y. Tsai Effect of hydroxypropyl-b-cyclodextrin complexation on the aqueous solubility, structure, thermal stability,

antioxidant activity, and tyrosinase inhibition of paeonol J. Incl. Phenom. Macrocycl. Chem., 72 (2012), pp. 405-411, 10.1007/s10847-011-0003-x

[44] J. Yaser, S. Hossein, R. Mahdi Stability and loading properties of curcumin encapsulated in Chlorella vulgaris Food Chem., 211 (2016), pp. 700-706, 10.1016/j.foodchem.2016.05.115

Figures

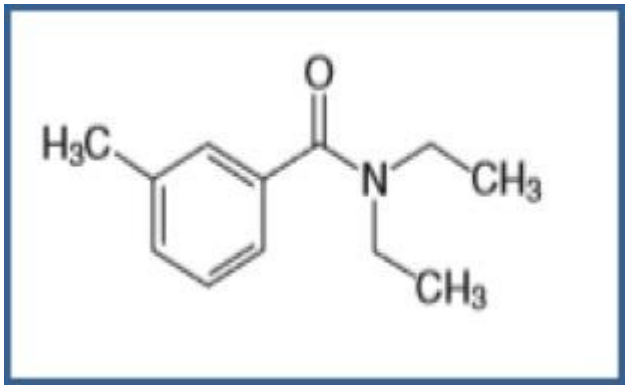

Fig. 1. Molecular structure of DEET.

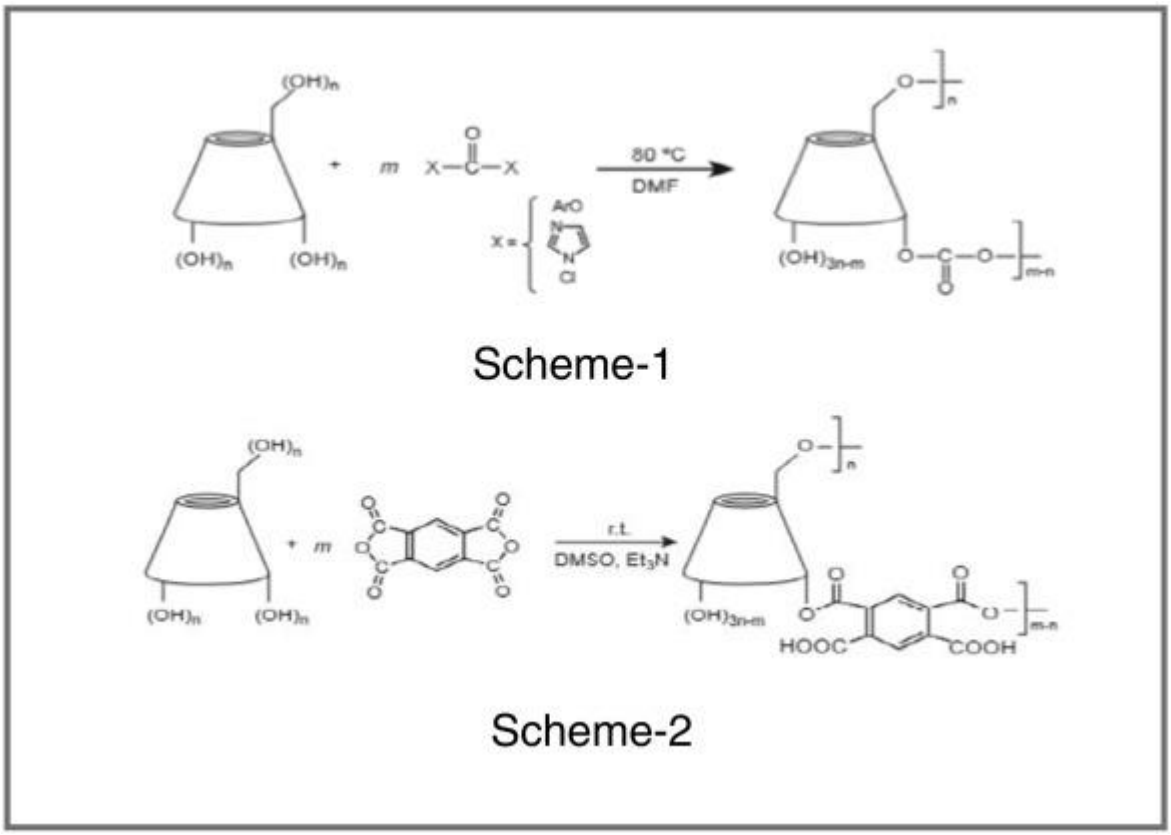

Fig. 2. Schemes of reactions –. Schematic representation of the reaction between CDI and β-cyclodextrin (scheme - 1) and between PMDA and β-cyclodextrin (scheme - 2).

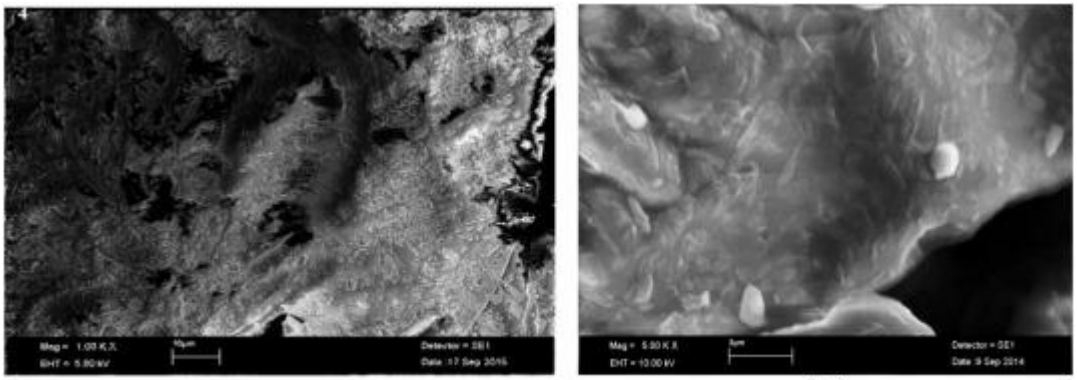

(A) (B)

Fig. 3. SEM images of DEET-loaded CDI-NSs (A) and PMDA-NSs (B).

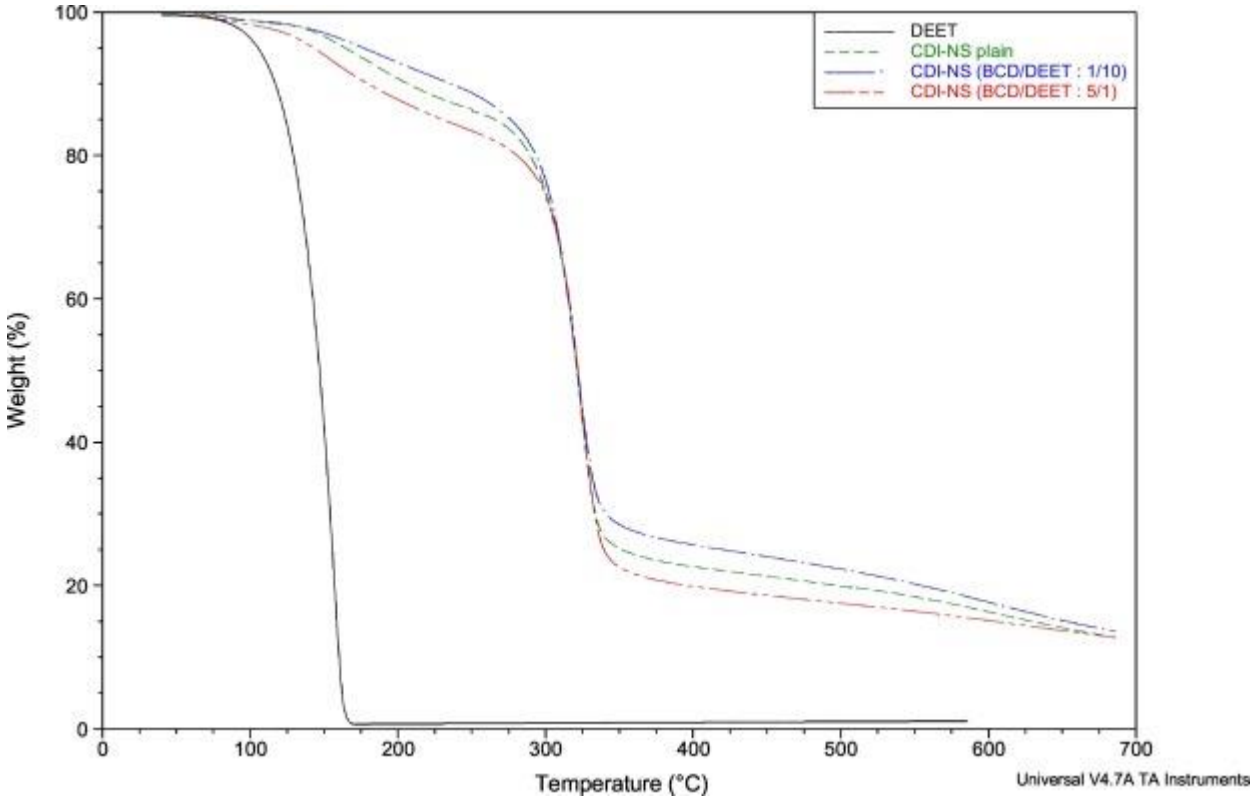

Fig. 4. TGA analysis of DEET, plain NSs, and DEET-laoded CDI-NSs.

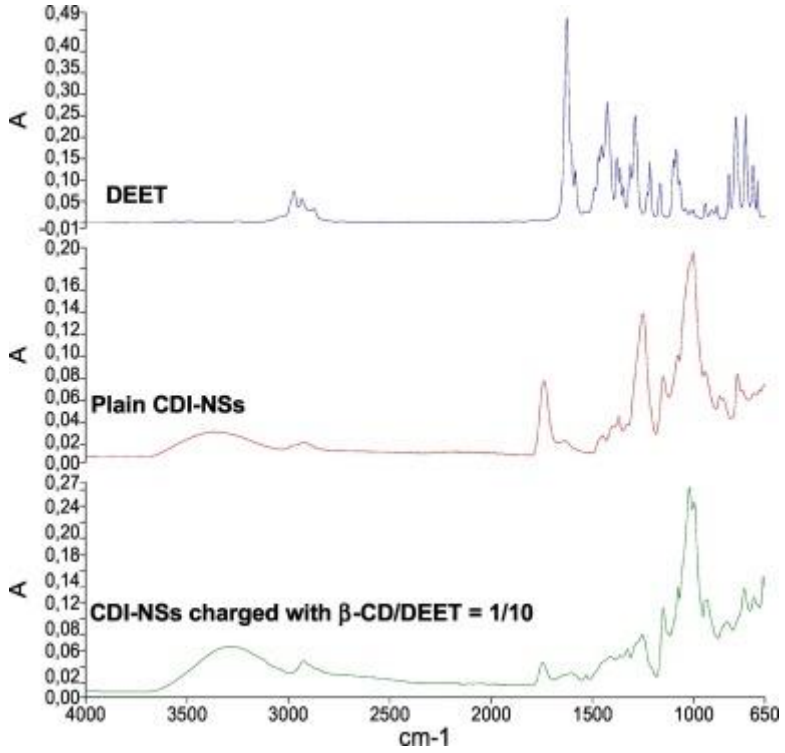

Fig. 5. FTIR spectra of DEET (blue line), plain CDI-NSs (red line), and DEET-loaded CD-NSs with 1:10 β-CD:DEET.

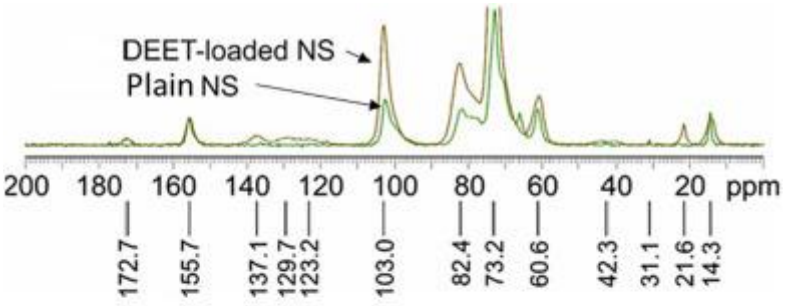

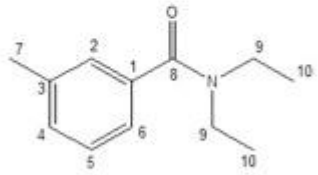

^{13}C SSNMR Assignments	
Chemical shift (ppm)	Assignment
172.7	8
155.7	NS
137.1	1/3
129.7	2/4/5
123.2	6
103.0	NS
82.4	NS
73.2	NS
60.6	NS
42.3	9
31.1	impurity
21.6	7
14.3	10/NS

Fig. 6. ^{13}C CPMAS NMR (0–200 ppm) spectra of plain CDI-NSs (1:8) and DEET-loaded CDI-NSs acquired with a spinning rate of 12 kHz at room temperature.

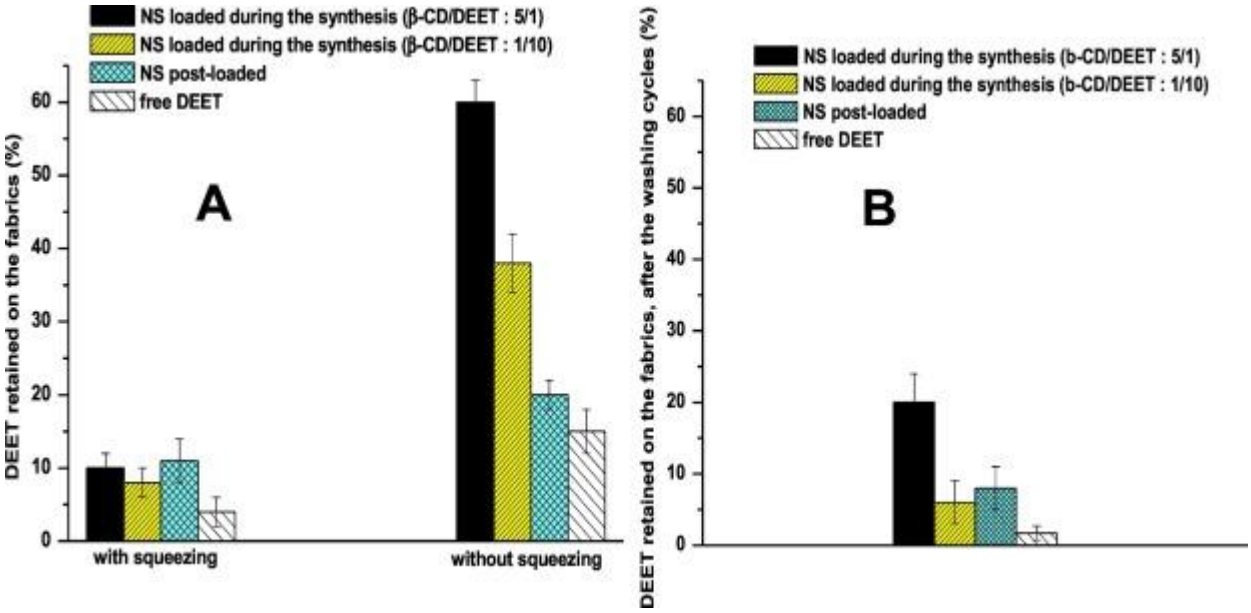

Fig. 7. DEET extraction from the functionalized fabrics, according to the different methodologies of functionalization before (A) and after washing, without sqeezeing (B).

Tables

Table 1. Operative parameters of CDI-and PMDA-NS synthesis.

β-CD:DEET	β-CD:CDI	CL	T (°C)[a]
Pre-loaded NS			
1:1	1:8	CDI/PMDA	RT/40/70
5:1	1:8	CDI/PMDA	RT/40/70
10:1	1:8	CDI/PMDA	RT/40/70
1:1	1:4	CDI/PMDA	RT/40/70
5:1	1:4	CDI/PMDA	RT/40/70
10:1	1:4	CDI/PMDA	RT/40/70
Post-loaded NS			
–	1:4	CDI/PMDA	RT/70
–	1:8	CDI/PMDA	RT/70

[a]Room Temperature (RT) for PMDA synthesis, 40–70 °C for CDI synthesis.

Table 2. DEET encapsulation efficiency and loading capacity of synthesized NSs.

β-CD:DEET molar ratio	CL	β-CD:CL molar ratio	T [°C]	EE [%]	LC [mg/g]
1:1	CDI	1:8	70	16.2 ± 3	20.0 ± 0.8
1:1	CDI	1:8	40	14.0 ± 5	14.2 ± 1.3
5:1	CDI	1:8	70	42.3 ± 4	11.8 ± 1.2
5:1	CDI	1:8	40	42.0 ± 4	11.4 ± 1.1
10:1	CDI	1:8	70	35.5 ± 3	4.9 ± 1.1
10:1	CDI	1:8	40	36.1 ± 3	5.1 ± 0.7
1:1	CDI	1:4	70	23.8 ± 2	5.1 ± 0.5
5:1	CDI	1:4	70	33.0 ± 4	9.8 ± 1.2
10:1	CDI	1:4	70	26.9 ± 3	4.5 ± 0.9
1:10	CDI	1:8	70	49.3 ± 2	291.0 ± 1.6
5:1 (post-loaded)	CDI	1:8	70	20.9 ± 3	5.8 ± 1.5
1:1	PMDA	1:8	RT	1.2 ± 4	0.5 ± 0.2
5:1	PMDA	1:8	RT	2.3 ± 4	0.3 ± 0.1
10:1	PMDA	1:8	RT	11.0 ± 3	0.7 ± 0.2
1:1	PMDA	1:4	RT	1.7 ± 2	0.6 ± 0.2
5:1	PMDA	1:4	RT	2.1 ± 3	0.4 ± 0.2
10:1	PMDA	1:4	RT	10.3 ± 2	0.6 ± 0.1

Table 3. BET analysis results: CDI-NS specific surface area, specific porous volume, and mean pores diameter.

	Sbet (m^2/g)	**Vp (cm^3/g)**	**Dp (Å)**
CDI-NSs (1:4)	0.836	0.002	71
CDI-NSs (1:8)	0.903	0.0014	58